Model incorporating deposition, diffusion, and aggregation in submonolayer nanostructures

Pablo Jensen,* Albert-László Barabási, Hernán Larralde,† Shlomo Havlin,‡ and H. E. Stanley
Center for Polymer Studies and Department of Physics, Boston University, Boston, Massachusetts 02215
(Received 9 December 1993)

We propose a model for describing diffusion-controlled aggregation of particles that are continually deposited on a surface. The model incorporates deposition, diffusion, and aggregation. We find that the diffusion and aggregation of randomly deposited particles "builds" a wide variety of fractal structures, all characterized by a common length scale L_1. This length L_1 scales as the ratio of the diffusion constant over the particle flux to the power $\frac{1}{4}$. We compare our results with several recent experiments on two-dimensional nanostructures formed by diffusion-controlled aggregation on surfaces.

PACS number(s): 68.70.+w, 68.35.Fx, 61.43.Hv, 68.35.Bs

Understanding the processes underlying the growth of thin films has led to widespread interest both from the physical and technological points of view [1,2]. *Equilibrium* ("thermodynamic") models have been developed and applied with some success to the film-substrate system [3]. However, recent dramatic improvements in experimental techniques, such as scanning tunneling microscopy, permit investigation of atomic details of the embryonic "submonolayer" stages of nanostructure film growth, and recent experimental work [4] has recognized the importance of *out of equilibrium* (kinetic) effects on the determination of the observed morphologies.

Addressing such out-of-equilibrium effects is important if one is to be able to control the morphology of submonolayer nanostructures. There exists some recent research on out-of-equilibrium models; for example, models such as percolation have been developed to describe surface deposition [5,6]. However, percolation assumes that the deposited particles do not diffuse after being deposited, when in fact not only diffusion but also aggregation of the diffusing particles takes place. There also exist models of diffusing particles that aggregate, but such "cluster-cluster aggregation" (CCA) models [7] do not incorporate the possibility of continual injection of new particles via deposition.

In this Brief Report, we propose an *out-of-equilibrium* model that incorporates simultaneously three phenomena not previously included in a single model: deposition, diffusion, and aggregation (DDA). The DDA model is defined as follows.

(a) Deposition. Particles are deposited at randomly chosen positions of the surface at a flux F per lattice site per unit time.

(b) Diffusion. A cluster of connected particles is chosen at random and moved north, east, south, or west by one lattice constant per unit time with a probability proportional to its mobility, which is given by $D_s = D_1 s^{-\gamma}$ [8]. Here s is the number of particles in the cluster, D_1 is the diffusion coefficient for a monomer ($s = 1$), and the parameter γ characterizes the dependence of D_s on cluster size.

(c) Aggregation. If two particles come to occupy neighboring sites, they (and therefore the clusters to which they belong) stick irreversibly [10].

Physically, it is not the flux but rather the normalized flux $\Phi \equiv F/D_1$ that tunes the relative strength of deposition and diffusion. For high fluxes ($\Phi \gg 1$), diffusion becomes negligible and we recover the classical static percolation model. The question is how to understand what happens when diffusion becomes important. We simulate our model on a square lattice with periodic boundary conditions. We fix Φ and the system size L, and follow the time evolution of the system until a spanning cluster appears. We call this final time the "spanning time."

For a fixed flux, the morphology of the system changes as a function of the system size. Figure 1 shows the dependence of the "total coverage" and the "spanning cluster coverage" as functions of the system size *at the spanning time*; the total coverage is defined as the total number of occupied sites divided by L^2 and the span-

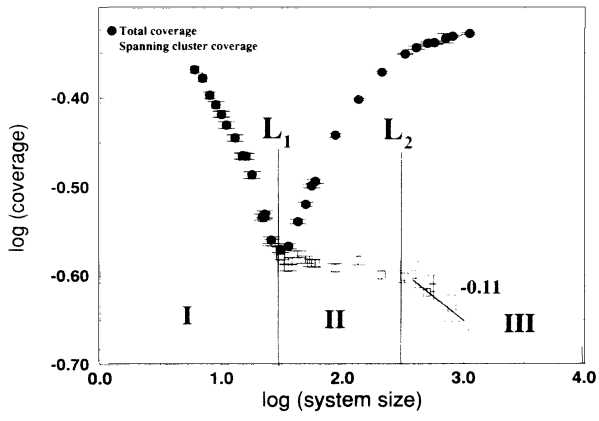

FIG. 1. Evolution of the total and spanning cluster coverages at the spanning time as a function of the system size; here $\gamma = 1$. We find three regimes of behavior (I, II, and III), delimited by two length scales L_1 and L_2. For this figure, the flux is $\Phi = 10^{-4}$.

*Permanent address: Département de Physique des Matériaux, Université Claude Bernard Lyon-1, Villeurbanne Cedex, France.

†Permanent address: Physics Department, Cavendish Laboratory, Cambridge University, Madingley Road, Cambridge CB3 0HE England.

‡Permanent address: Physics Department, Bar Ilan University, Ramat Gan, Israel.

ning cluster coverage as the number of sites of the spanning cluster divided by L^2. We find three characteristic regimes, delimited by two crossover length scales L_1 and L_2: L_1 is the characteristic diffusion length of a single particle on the surface, while L_2 emerges from the competition between deposition and *cluster* diffusion.

Regime I ($L < L_1$): "Particle diffusion regime." In this regime, only one cluster is present in the system. This is seen in Figs. 2(a) and 2(b) and is also supported by Fig. 1: the total and spanning cluster coverages are superposed. Since the characteristic diffusion length of a single particle L_1 is larger than the system size L, every deposited particle attaches to the already existing cluster before the next particle is deposited. At short times, the cluster is small and virtually all the particles are deposited outside the cluster and reach it by Brownian diffusion, so we expect that the cluster should have features in common with DLA. Indeed, at short times, we find that the cluster resembles DLA [Fig. 2(a)]. Its fractal dimension, measured by the sandbox method [2] is found to be 1.7, in agreement with the expected value for a DLA cluster [2]. At longer times, when the size of the cluster becomes comparable to the system size, a larger fraction of particles are deposited *inside* the cluster. Therefore, the model cannot be precisely the same as DLA; e.g., at the time of spanning, almost all new particles are deposited inside the boundaries of the cluster [cf. Fig. 2(b)].

Regime II ($L_1 < L < L_2$): "Cluster diffusion regime." Now several clusters are present in the system, as can be seen in Figs. 2(c) and 2(d). This can also be inferred from Fig. 1: at L_1 the curves for the different coverages split, indicating that, in addition to the spanning cluster, there are other clusters contributing to the total coverage. The reason for this is that the diffusion length is now smaller than the system size, so that several clusters nucleate on the surface. These clusters are separated by the distance set by the diffusion length L_1. We find that the spanning cluster is mainly built by the accretion of the diffusing nucleating clusters [Fig. 2(d)].

Regime III ($L > L_2$): "Percolation regime." At short times, many clusters are present in the system [Fig. 2(e)] and they are separated, as in regime II, by a distance L_1. At the spanning time, the system resembles a percolation network [Fig. 2(f)]. The fractal dimension of the clusters as measured by the sandbox method is close to 1.9, corresponding to the value of percolation clusters [2]. This can also be seen in Fig. 1 from the slope of the spanning cluster coverage as a function of the system size. Moreover, in this regime only, we find that the total coverage

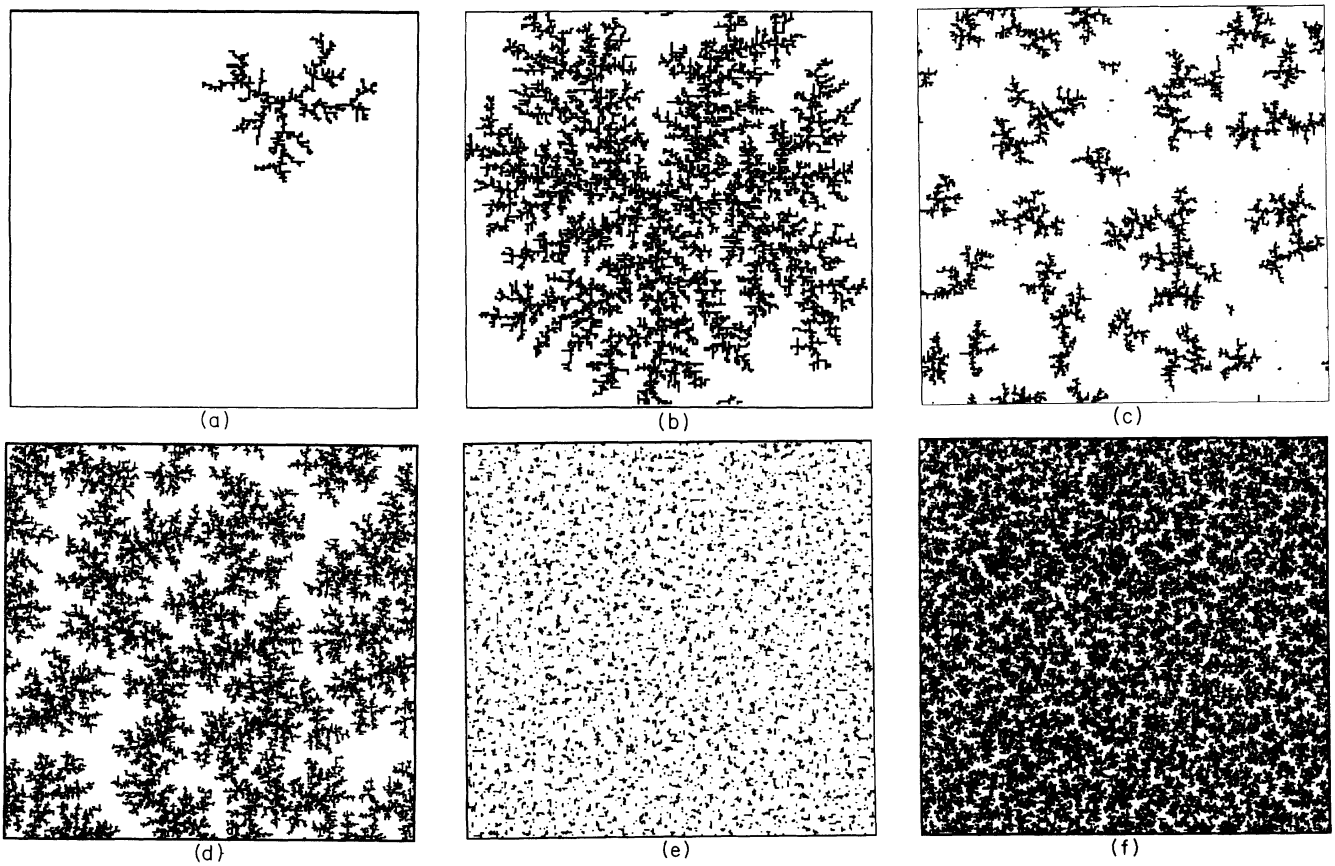

FIG. 2. System morphologies in the three regimes: (a) and (b) regime I, (c) and (d) regime II, and (e) and (f) regime III. *Regime I (system size smaller than L_1)*: shown are two stages of the growth for $\Phi = 10^{-9}$ ($L_1 \simeq 500$) and $L = 200$. (a) Total coverage, 0.02; (b) spanning point: total coverage, 0.27. *Regime II (system size between L_1 and L_2)*: shown are two stages of the growth for $\Phi = 10^{-6}$ ($L_1 \simeq 90$ and $L_2 \simeq 10^4$) and $L = 300$. (c) Total coverage, 0.1; (d) spanning point: total coverage, 0.31. *Regime III (system size larger than L_2)*: shown are two stages of the growth for $\Phi = 10^{-3}$ ($L_1 \simeq 17$ and $L_2 \simeq 36$) and $L = 300$. (e) Total coverage, 0.1; (f) spanning point: total coverage, 0.49. For all six figures, we choose $\gamma = 1$.

scales with the system size as $p_c(L) - p_c(\infty) \sim L^{-1/\nu}$, with $\nu \simeq 1.3$, which is in good agreement with the exponent 4/3 predicted by percolation [2].

Figure 1 shows results obtained for the flux $\Phi=10^{-4}$, but similar results have been obtained for the other fluxes we have studied ($10^{-6} \leq \Phi \leq 10^{+5}$). We find that a change of the flux affects the values of the two crossover lengths L_1 and L_2. We have determined L_1 and L_2 for several different fluxes: the results are presented in Fig. 3. The dependence of L_1 on Φ can be understood by noting that the time needed by a single deposited particle randomly diffusing to explore the whole system is proportional to the system area and inversely proportional to the diffusion coefficient: $t_{dif} \simeq L^2/D_1$. By definition of the flux, the average time at which another particle is added to the system is $t_{dep} = 1/(FL^2)$. If $t_{dif} \ll t_{dep}$, the particle has sufficient time to explore the whole system (and therefore find an already existing cluster) before another particle is added. Consequently, a single cluster is built. If $t_{dif} \gg t_{dep}$, the particle finds another deposited particle before having had time to explore the whole system. Then several clusters are formed: this corresponds to regime II. The crossover between the two regimes occurs when these two times become comparable. This occurs for

$$L_1 \sim \Phi^{-\psi_1}, \tag{1}$$

where $\psi_1 = 1/4$, in excellent agreement with the numerically obtained exponent of 0.24 ± 0.02 (Fig. 3). L_1 can be interpreted as the length scale determined by the competition between particle deposition (t_{dep}) and *single* particle diffusion (t_{dif}).

The second length scale L_2 also scales with the flux

$$L_2 \sim \Phi^{-\psi_2}, \tag{2}$$

where $\psi_2 = 0.9 \pm 0.2$ for $\gamma = 1$. We find that ψ_2 decreases as γ increases, unlike ψ_1, which is independent of γ. To uncover a physical interpretation of L_2, we fix the flux and change the system size. For spanning to occur, we must grow a cluster of size comparable to the system size. If the system is large, the clusters become large and therefore their diffusion coefficient becomes extremely small. In this limit, deposition dominates and connects the system in a percolationlike way. For smaller systems, the clusters are also smaller; they can move and connect one another to build clusters of sizes comparable to that of the system. Then diffusion dominates the connectivity of the system. The boundary between these two system sizes is set by L_2. Then, L_2 can be interpreted as the length scale determined by the competition between particle deposition and *cluster* diffusion. This analysis is supported by the fact that the second crossover L_2 is not observed when only single particles are allowed to move, thereby suppressing the possibility that the connections are made by cluster diffusion.

Based on the previous results, we may now construct a "morphology phase diagram" that serves to characterize the morphology of the system at the spanning time in terms of the two tuning parameters L and Φ (Fig. 3). The three regimes I–III are delineated by the two crossover lines $L_1(\Phi)$ and $L_2(\Phi)$, which intersect at a "critical point" whose coordinates (Φ_c, L_c) depend only on γ. Thus for a fixed system size L, two situations can arise, depending on the value of γ. (i) If $L \ll L_c(\gamma)$, then the system shows a direct transition from the single cluster regime to percolation as the normalized flux Φ increases. (ii) If $L \gg L_c(\gamma)$, then regime II can also be observed for intermediate values of the normalized flux.

In summary, we have proposed a model for describing diffusion-controlled aggregation of particles that are continually deposited on a surface. The model, which incorporates deposition, diffusion, and aggregation, is motivated by recent thin film deposition experiments using

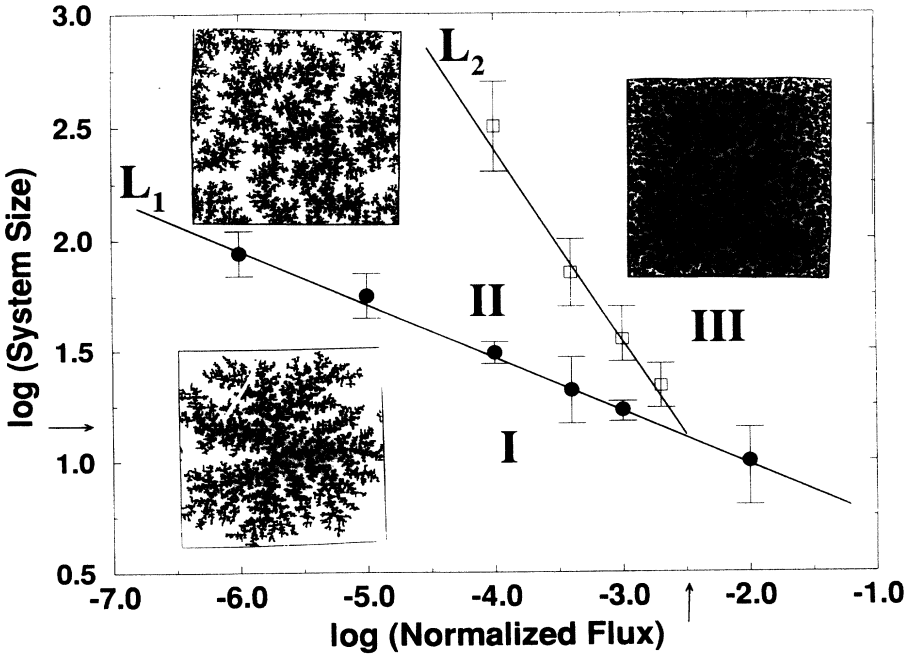

FIG. 3. The (Φ, L) phase diagram for $\gamma = 1$. Shown is the dependence on normalized flux of the two length scales L_1 (full circles) and L_2 (open squares). The lines separating the three regimes I–III have been obtained by linear fits of the data for L_1 (slope $\psi_1 = 0.24 \pm 0.02$) and L_2 (slope $\psi_2 = 0.9 \pm 0.2$). The arrows indicate the critical values Φ_c and L_c. The insets show typical morphologies for each regime.

the low-energy cluster beam deposition (LECBD) technique [5]. Indeed, the structures obtained in Figs. 2(c) and 2(e) (low coverages) resemble some experimental images obtained by LECBD (see Fig. 3 of [6]) on substrates held at low temperatures. We find that the model permits one to distinguish the effects of deposition, diffusion, and aggregation and that tuning the relative strength of, e.g., deposition and diffusion, generates a rich range of morphologies, including diffusion limited aggregation, CCA, and percolation. The length and time scales characterizing these morphologies depend on experimentally controllable parameters such as deposition flux and diffusion constant, raising the possibility that the model may prove useful in future studies seeking controlled design of nanostructure morphologies. We hope that the model may be useful in many situations where diffusion and aggregation occur in the presence of continuous deposition.

Note added. After this work was completed, Röder *et al.* [11] published a series of remarkable experiments documenting the formation of nanometer-scale surface structures. Our model mimics the same process and produces morphologies that remarkably resemble the experimental structures [e.g., Fig. 2(c) bears a striking similarity to Fig. 1d of [11]]. Also, after this work was submitted, we learned of a careful study [12,13] that treats a related model in which clusters do not diffuse. We recently learned that $\psi_1 = \frac{1}{4}$ has been derived in a more general context in connection with studies on atomic diffusion during MBE growth [14].

We wish to thank C. Henry, J. Kertész, D. Stauffer, and A. Vespignani for helpful discussions and P. J. Feibelman for several insightful remarks. P.J. acknowledges CNRS and NATO for financial support. H.L. thanks CONACYT, Mexico, for support. A.-L.B. and H.E.S. thank the Hungary–U.S. exchange program of the Hungarian Academy of Sciences. S.H. acknowledges the U.S.–Israel Binational Science Foundation for financial support. The Center for Polymer Studies is supported by the NSF.

[1] P. Meakin, Rep. Prog. Phys. **55**, 157 (1992); *Surface Disordering: Growth, Roughening, and Phase Transitions*, Proceedings of the 1992 Les Houches Workshop, R. Jullien, J. Kertész, P. Meakin, and D. E. Wolf (Nova Science, New York, 1992).

[2] T. Vicsek, *Fractal Growth Phenomena*, 2nd ed. (World Scientific, Singapore, 1992).

[3] J. A. Venables, G. D. T. Spiller, and M. Hanbücken, Rep. Prog. Phys. **47**, 399 (1984).

[4] R. Q. Hwang, J. Schröder, C. Günther, and R. J. Behn, Phys. Rev. Lett. **67**, 3279 (1991).

[5] P. Melinon, P. Jensen, J. X. Hu, A. Hoareau, B. Cabaud, M. Treilleux, and D. Guillot, Phys. Rev. B **44**, 12 562 (1991).

[6] P. Jensen, P. Melinon, A. Hoareau, J. X. Hu, B. Cabaud, M. Treilleux, E. Bernstein, and D. Guillot, Physica A **185**, 104 (1992).

[7] P. Meakin, Phys. Rev. Lett. **51**, 1119 (1983); M. Kolb, R. Botet, and R. Jullien, *ibid.* **51**, 1123 (1983); for a comprehensive review, see H. J. Herrmann, Phys. Rep. **136**, 153 (1986).

[8] In MBE, *rigid* cluster diffusion is not expected. Only monomers and dimers have non-negligible diffusion constants. We can reach this limit in the present model by choosing the tunable parameter γ to be large. However, for some systems there is experimental evidence that the diffusion coefficient of clusters of size N varies as $D_N = D_0 N^{-2/3} \exp(-E_a/k_B T)$, which gives $\gamma = 2/3$ [9]. The finite γ case, on which we focus in this paper, is most relevant for these systems.

[9] C. Chapon and CR Henry, Surf. Sci. **106**, 152 (1981); C. Reiners, Thin Solid Films, **143**, 311 (1986).

[10] The diffusion of the adatoms on the edge of the clusters is neglected in the present "zeroth order" model. Indeed, at low temperatures edge diffusion is probably not relevant, due to the activated nature of the diffusion process. However, at higher temperatures, edge diffusion may influence cluster morphology. We intend to take into account edge diffusion in future work on this model.

[11] H. Röder, E. Hahn, H. Brune, J.-P. Bucher, and K. Kern, Nature **366**, 141 (1993); P. Jensen, A.-L. Barabási, H. Larralde, S. Havlin, and H. E. Stanley, in Proceedings of the 1993 ETOPIM-3 Conference [Physica A **207**, 219 (1994)]; Nature **368**, 22 (1994).

[12] L.-H. Tang, J. Phys. (Paris) I **3**, 935 (1993); J. Villain, A. Pipinelli, L.-H. Tang, and D. E. Wolf, *ibid.* **2**, 2107 (1992); J. Villain, A. Pipinelli, and D. E. Wolf, Phys. Rev. Lett. **69**, 985 (1992).

[13] J. G. Amar, F. Family, and P-M Lam, Phys. Rev. B (to be published).

[14] S. V. Ghaisas and S. Das Sarma, Phys. Rev. B **46**, 7308 (1992).

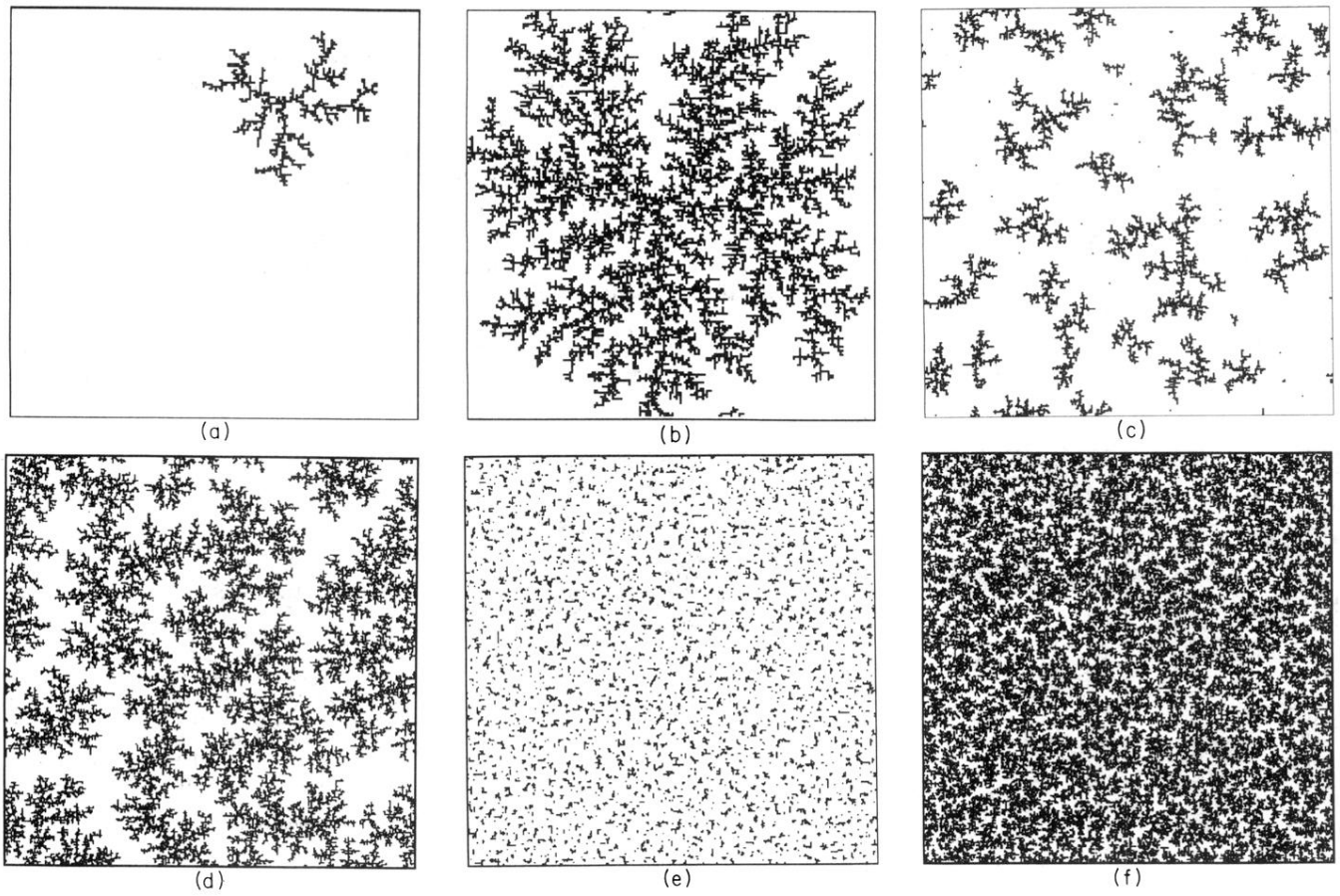

FIG. 2. System morphologies in the three regimes: (a) and (b) regime I, (c) and (d) regime II, and (e) and (f) regime III. *Regime I (system size smaller than L_1)*: shown are two stages of the growth for $\Phi = 10^{-9}$ ($L_1 \simeq 500$) and $L = 200$. (a) Total coverage, 0.02; (b) spanning point: total coverage, 0.27. *Regime II (system size between L_1 and L_2)*: shown are two stages of the growth for $\Phi = 10^{-6}$ ($L_1 \simeq 90$ and $L_2 \simeq 10^4$) and $L = 300$. (c) Total coverage, 0.1; (d) spanning point: total coverage, 0.31. *Regime III (system size larger than L_2)*: shown are two stages of the growth for $\Phi = 10^{-3}$ ($L_1 \simeq 17$ and $L_2 \simeq 36$) and $L = 300$. (e) Total coverage, 0.1; (f) spanning point: total coverage, 0.49. For all six figures, we choose $\gamma = 1$.

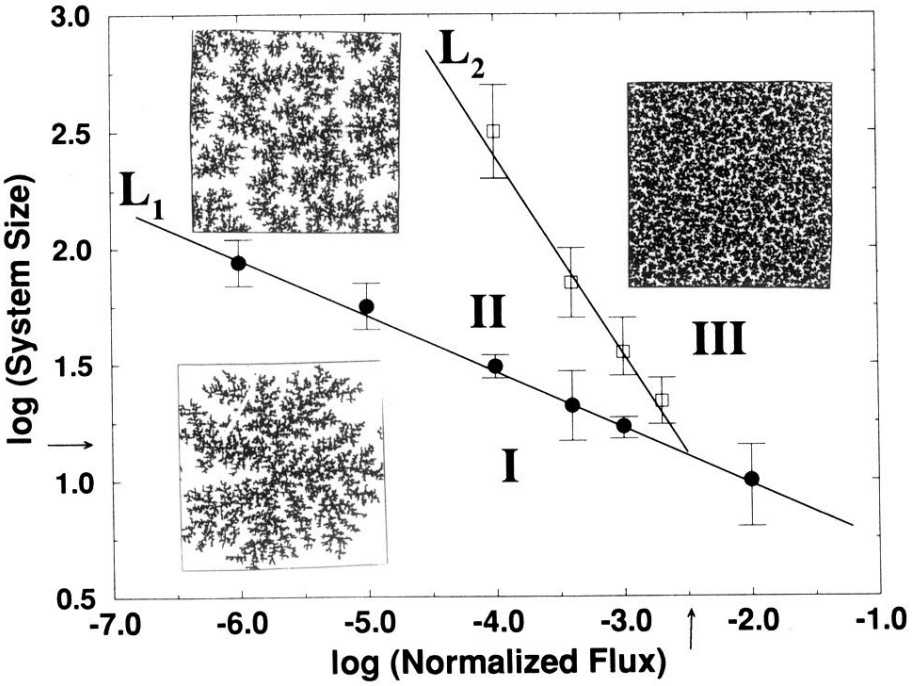

FIG. 3. The (Φ, L) phase diagram for $\gamma = 1$. Shown is the dependence on normalized flux of the two length scales L_1 (full circles) and L_2 (open squares). The lines separating the three regimes I–III have been obtained by linear fits of the data for L_1 (slope $\psi_1 = 0.24 \pm 0.02$) and L_2 (slope $\psi_2 = 0.9 \pm 0.2$). The arrows indicate the critical values Φ_c and L_c. The insets show typical morphologies for each regime.